H1-04/99-571

Absolute hadronic jet calibration of the H1 liquid Argon calorimeter

M. Jacquet[1], **Z. Zhang**[1]

and

V. Brisson[1], **S. Kermiche**[2], **C. Vallée**[2]

1: LAL (Orsay), 2: CPPM (Marseille)

1 Introduction

The H1 liquid argon calorimeter (LAr) has the advantage of a very large stability with time. Nevertheless, the absorbing material for the hadronic part - stainless steel - is not "compensating", i.e. the response to electrons and pions is different. To overcome this drawback, weighting algorithms([1]), determined both from Monte Carlo and CERN test data, are applied to hadronic clusters to improve the measurements and the resolution. But even with this weighting procedure, the systematic uncertainty on the hadronic scale is still of the order of 5%. More refined comparisons have to be made between data and Monte Carlo in order to correct for effects due to imperfections and inhomogeneities of the different parts of the calorimeter. And still more important is to determine the absolute hadronic energy scale, which has not been reached yet, and is under-estimated by not at all negligeable factors.

The method presented here aims to obtain hadronic quantities measured in LAr with an absolute scale and a systematic uncertainty both better than 2%. The main principle of the method is to impose the balance between the transverse momenta of the positron and of the hadronic system. The technical implementation is described in appendix.

2 Calibration samples and selection

The samples used for this calibration contain all the high Q^2 neutral current events selected in the data taken from 1994 to 1997. For the Monte Carlo, two different hadronisation models have been used. The first Monte Carlo file has been generated with the CDM hadronic final state model (ARIADNE[2]) and the second one with the MEPS model (LEPTO[3]). The Monte Carlo events have been generated with $Q^2 > 90$ GeV^2, simulated and reconstructed under 1997 runing conditions.

2.1 Kinematics

The calibration is based on the AEFR scale[1]; all the quantities used in the following analysis are calculated from the AEFR bank which contains the measured energies of the calorimeter cells after weighting.

The quantity $\mathrm{pt_{had}}$ stands for the total hadronic transverse momentum, θ_{had} and $\theta^{\mathrm{e}}_{\mathrm{had}}$ for the hadronic inclusive polar angle calculated respectively with the hadronic and the positron variables:

$$\mathrm{pt_{had}} = \sqrt{\left(\sum_{\mathrm{h}} \mathrm{px_h}\right)^2 + \left(\sum_{\mathrm{h}} \mathrm{py_h}\right)^2}$$

$$\tan\frac{\theta_{\mathrm{had}}}{2} = \frac{\sum_{\mathrm{h}}(\mathrm{E_h} - \mathrm{pz_h})}{\mathrm{pt_{had}}} \qquad \tan\frac{\theta^{\mathrm{e}}_{\mathrm{had}}}{2} = \frac{2\mathrm{E_0} - (\mathrm{E_e} - \mathrm{pz_e})}{\mathrm{pt_e}}$$

where the summation h is over all energy deposits of the hadronic final states; $\mathrm{E^0_e}$, $\mathrm{E_e}$, $\mathrm{pz_e}$ and $\mathrm{pt_e}$ are respectively the energy of the incident positron, the energy, the longitudinal and transverse momenta of the scattered positron. In order to compute the calibaration coefficients and to check the method with two independent variables, θ_{had} will be used in the calibration procedure (sections 2 and 3) and $\theta^{\mathrm{e}}_{\mathrm{had}}$ in the check part (section 4).

For each event, jets have been recontructed with the QJCONE algorithm ([4]) in which the cone radius has been chosen as 1 rad and the minimum transverse jet momentum as 4 GeV; $\mathrm{pt_{jet_j}}$ and $\theta_{\mathrm{jet_j}}$ are the transverse momentum and the polar angle of the jet j:

$$\mathrm{pt_{jet_j}} = \sqrt{\left(\sum_{\mathrm{j}} \mathrm{px_j}\right)^2 + \left(\sum_{\mathrm{j}} \mathrm{py_j}\right)^2} \qquad \tan\frac{\theta_{\mathrm{jet_j}}}{2} = \frac{\sum_{\mathrm{j}}(\mathrm{E_j} - \mathrm{pz_j})}{\mathrm{pt_{jet_j}}}$$

[1] No intermediate dead material correction, e.g. AEDCORR, has been applied; this correction was derived from earlier data with limited statistical precision.

where the summation j is over all hadronic final state particles belonging to the reconstructed jet number j.

The total transverse momentum $\mathrm{pt_{DA}}$ is calculated with the double angle method from the angles of the positron and of the hadronic system:

$$\mathrm{pt_{DA}} = \frac{2\mathrm{E_e^0}}{\alpha_\mathrm{e} + \alpha_\mathrm{h}}$$

where $\alpha_\mathrm{e} = \tan(\theta_\mathrm{e}/2)$, $\alpha_\mathrm{h} = \tan(\theta_\mathrm{had}/2)$, and $\mathrm{E_e^0}$ is the energy of the incident positron.

The pt balance $\mathrm{pt_{bal}}$ stands for the ratio of the hadronic transverse momentum and the double angle transverse momentum:

$$\mathrm{pt_{bal}} = \frac{\mathrm{pt_{had}}}{\mathrm{pt_{DA}}}$$

2.2 Selection cuts

2.2.1 Selection for the calibration

To perform the hadronic energy calibration, the reference of the transverse momentum is decuced from double angle method. In order to have clean samples and good double angle momentum measurements, the following cuts have been applied on the data and Monte Carlo samples:

- 1 electron with $\mathrm{pt_e}$ >10 GeV
- only 1 jet
- good $\mathrm{pt_{DA}}$ measurement cuts:
  - $\mathrm{pt_e/pt_{DA}} > 0.88$
  - $\mathrm{E_{spacal}/E_{total}} < 1\%$
  - $\mathrm{pt_{spacal}/pt_{total}} < 1\%$
  - $\mathrm{d}\theta = (\theta_\mathrm{had} - \theta_\mathrm{jet})/\theta_\mathrm{jet} < 1.5$

where the first cut is applied to remove hard initial radiation events (ISR), in which the values of $\mathrm{pt_{DA}}$ are biased. The last cut is applied to obtain a good $\mathrm{pt_{DA}}$ measurement at low transverse momenta and very low jet angles where particles may be lost in the beam pipe. Fig.1 shows the effect of this cut on the CDM Monte Carlo sample: the double angle measurement is improved after the cut in the region ($\theta_\mathrm{jet} < 15^\mathrm{o}$ and pt<15 GeV).

It should be pointed out that no cut associated directly with the hadronic energy is applied in this calibration selection. Indeed, such cut would distort the pt balance distributions, especially at low pt (∼10-15 GeV), and would change the distribution means.

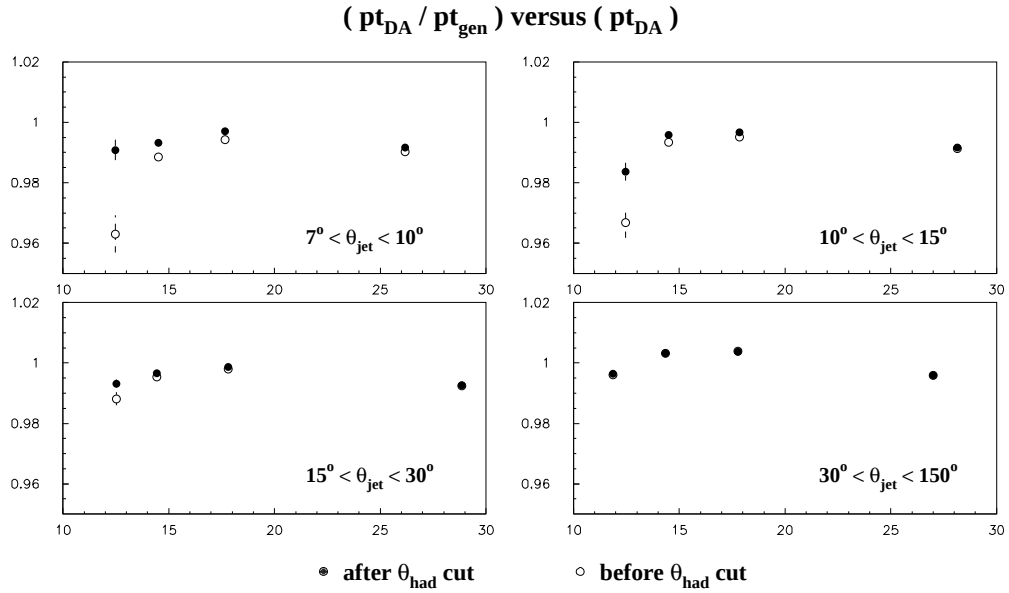

Figure 1: $\mathrm{pt_{DA}}/\mathrm{pt_{gen}}$ versus $\mathrm{pt_{DA}}$ in different θ_{jet} regions, for CDM 1+1 jet events, before and after dθ cut (all the other cuts applied).

Another point of concern is to check that the calibration procedure corrects only for the energy scale of the calorimeter and not for energy losses in the beam pipe. This is done in fig.2, which shows that for the calibration sample the transverse momentum flow generated in the acceptance of the calorimeter ($[\mathrm{pt_{det}}]_{\mathrm{gen}}$) is equal within 2% to the total transverse momentum ($\mathrm{pt^2_{gen}} = \mathrm{Q^2_{gen}}(1 - \mathrm{y_{gen}})$), whatever the direction of the hadronic system.

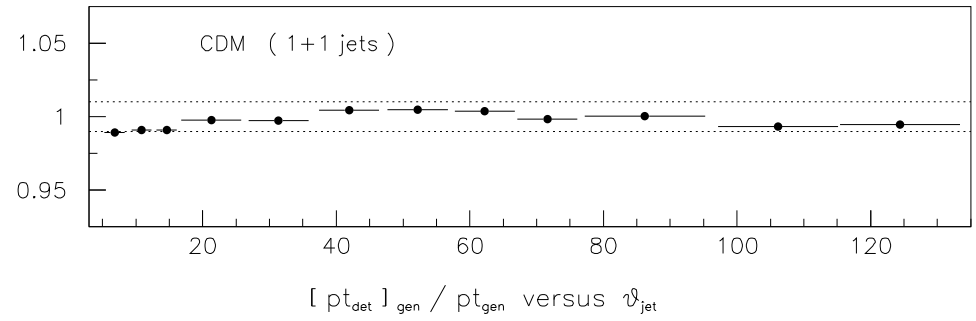

Figure 2: $[\mathrm{pt_{det}}]_{\mathrm{gen}}/\mathrm{pt_{gen}}$ versus θ_{jet} (based on the CDM sample, after calibration cuts).

Finally, Fig.3 shows a comparison between the double angle transverse momentum and the true transverse momentum for CDM and MEPS samples before and after the calibration selection cuts. After all the cuts, the pt_{DA} measurement is improved: the means of the pt_{DA}/pt_{gen} distributions are around unity and the tails are reduced.

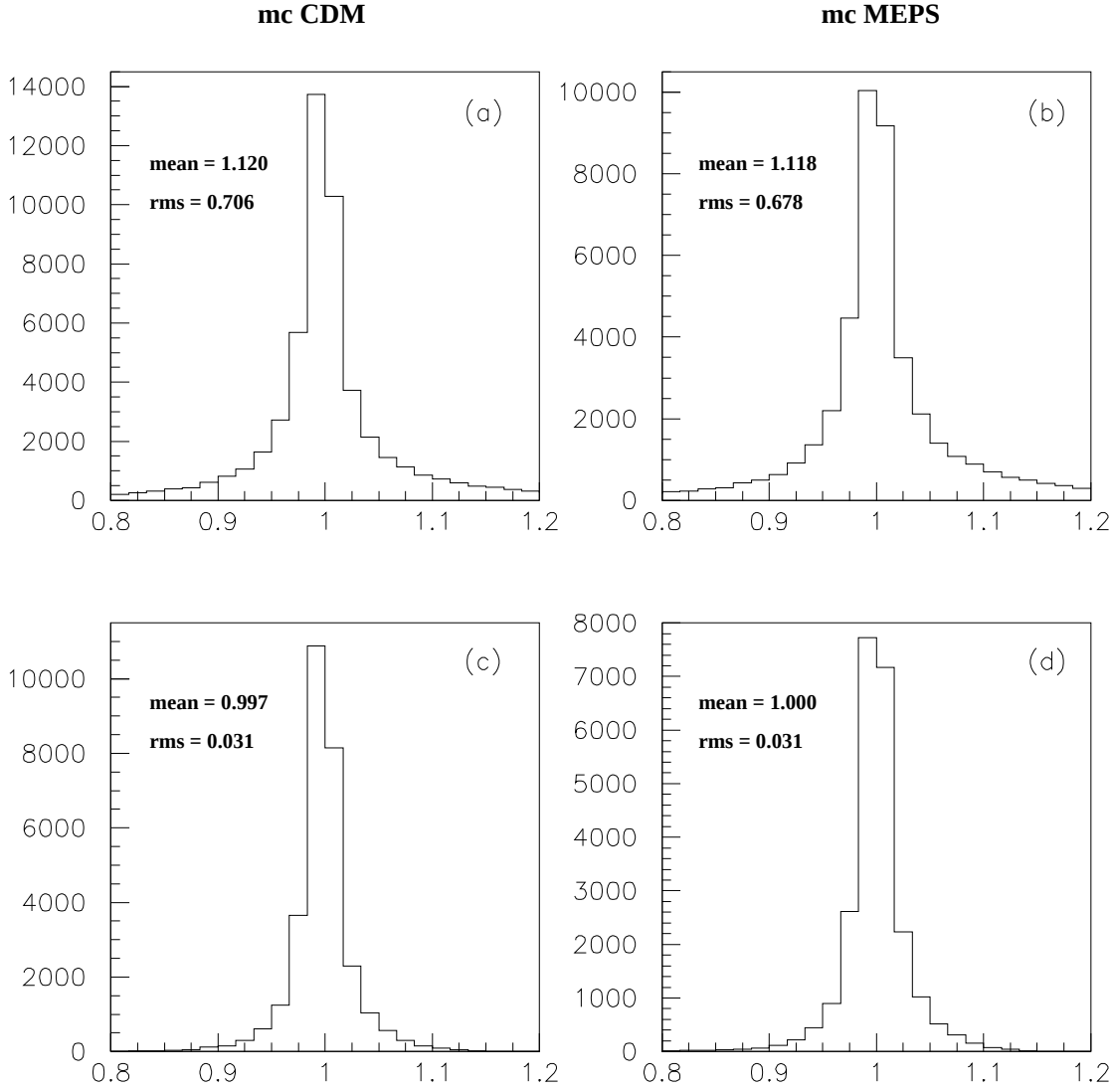

Figure 3: pt_{DA}/pt_{gen} for CDM and MEPS 1+1 jet events, before cuts [(a),(b)] and after cuts [(c),(d)] .

2.2.2 Selection for the checks

The cuts used to do various checks (section 4) are not the ones applied to calculate the corrections. This different set of cuts will allow to check that the method is not depending on the cuts used to compute the calibration coefficients and works also with a more standard cut set (which can contain hadronic energy cuts). The selection here, which is a more standard neutral current selection, is the following:

- 1 electron with $\mathrm{pt_e}$ >10 GeV,
- $\mathrm{pt_{had}}/\mathrm{pt_e} > 0.35$,
- $\sum_{\mathrm{h,e}} (\mathrm{E} - \mathrm{pz}) > 42$ GeV (anti ISR cut),
- $\theta_{\mathrm{jets}} > 7^{\mathrm{o}}$, this last cut ensuring that the jets are well contained in the calorimeter acceptance.

The two last cuts here allow again to have good $\mathrm{pt_{DA}}$ measurements.

To be clearer in the following, Table 1 gives the number of events of the different data selections and the corresponding Monte Carlo samples[2].

SAMPLE NAME	**# of jets**	**DATA**	**CDM**	**MEPS**
1+1 jet calib sample	1+1	50560	26174	21488
inclusive check sample	any #	80213	41388	35048
1+1 jet check sample	1+1	64257	32620	27195
1+2 jet check sample	1+2	13487	7190	6036
1+3 jet check sample	1+3	2175	1330	1472

Table 1: Statistics in the different selected samples used.

[2]In the future, new Monte Carlo samples generated at larger Q^2 will be added to have a Monte Carlo statistics larger than the data statistic, and to perform and test the calibration at very high Q^2.

3 Calibration procedure

With the 1+1 jet calibration samples defined in the previous section, the calibration procedure is performed in two steps. In the first step, a relative calibration between the data and the Monte Carlo's is made to correct possible detector effects while, in the second step, an absolute hadronic energy scale is achieved both in the data and in Monte Carlo's by imposing the pt balance between the scattered positron and the hadrons.

3.1 Step 1: relative calibration

For this step one, the data and the Monte Carlo's are compared in the different wheels of the calorimeter; a wheel is defined here by the polar jet angle. More precisely, the ratio:

$$(\mathrm{pt_{bal}})^{\mathrm{Data}} \ / \ (\mathrm{pt_{bal}})^{\mathrm{Monte\ Carlo}}$$

is computed in different θ_{jet} ranges, corresponding to roughly various physical calorimeter wheels. The azimuthal angle dependence, which had been found not significant, is not taken into account. The statistical means of these distributions are presented in Table 2 as a function of θ_{jet} when the data are compared with the CDM Monte Carlo and with the MEPS one:

$\theta_{\mathbf{jet}}$ **range**	**DATA/CDM**	**DATA/MEPS**
<15°	0.977 ± 0.002	0.987 ± 0.003
15-30°	0.958 ± 0.002	0.964 ± 0.002
30-42°	0.965 ± 0.003	0.979 ± 0.003
42-55°	0.972 ± 0.004	1.007 ± 0.004
55-80°	0.992 ± 0.003	1.017 ± 0.003
80-110°	0.993 ± 0.004	1.027 ± 0.004
110-135°	0.990 ± 0.006	1.027 ± 0.006
135-155°	1.080 ± 0.018	1.065 ± 0.020

Table 2: Step 1: relative calibration coefficients.

As said above, the coefficients are determined from the statistical mean of each pt balance ratio distribution; but these corrections can be determined as well from a Gaussian fit of each distribution: the difference of the two methods is at the level of a few per mil, therefore negligible compared to the correction itself.

3.2 Step 2: absolute calibration

The second step is devoted to obtain an absolute hadronic energy scale. Data and Monte Carlo's are corrected separately, taking the double angle transverse momentum as a reference. This calibration step is done, as in step 1, as a function of the jet angle $\theta_{\rm jet}$, but also here as a function of $\rm pt_{DA}$.

The $\theta_{\rm jet}$ bins which have been chosen slightly different from that of step 1[3] are listed below:

$\mathbf{IF_1}$	$\mathbf{IF_2}$	**OF**	**FB**	**CB3**	**CB2**	**CB1**	**BBE**
7-10^o	10-15^o	15-30^o	30-55^o	55-80^o	80-110^o	110-135^o	135-155^o

In each wheel, the pt balance is computed in several $\rm pt_{DA}$ ranges. Each statistical mean of these distributions is extracted and the resulting points are fitted with an exponential function $\rm F(\theta_{jet}, pt_{DA})$, the expression of which is given by:

$$\rm F(\theta_{jet}, pt_{DA}) \;=\; A_\theta \;[\; 1 \;-\; \exp(-B_\theta - pt_{DA}/C_\theta) \;]$$

Fig.4 (resp. Fig.5) shows these pt balance mean points versus $\rm pt_{DA}$ in the different wheels for the data already corrected by the CDM (resp. MEPS) step 1 coefficients, and for the CDM (resp. MEPS) Monte Carlo. The fitted functions obtained are also drawn. Table 3 shows the results of these fits for the data and for the two Monte Carlo's in each $\theta_{\rm jet}$ range.

As described in this section, two different sets of correction functions have been computed for the two Monte Carlo models. Indeed, it will be shown in section 4 that the MEPS and CDM models lead to different hadronic system behaviours and that only one calibration is not sufficient to correct the two at the 2% level. Obviously, this implies also two set of calibration coefficients for the data, as the step 1 relative calibration constants are obtained with respect to a given Monte Carlo model. However, because of the compensation between the two steps, the overall calibration correction for data does not depend on any Monte Carlo model. It's only for indication that the two are given.

[3]For comparison with another analysis

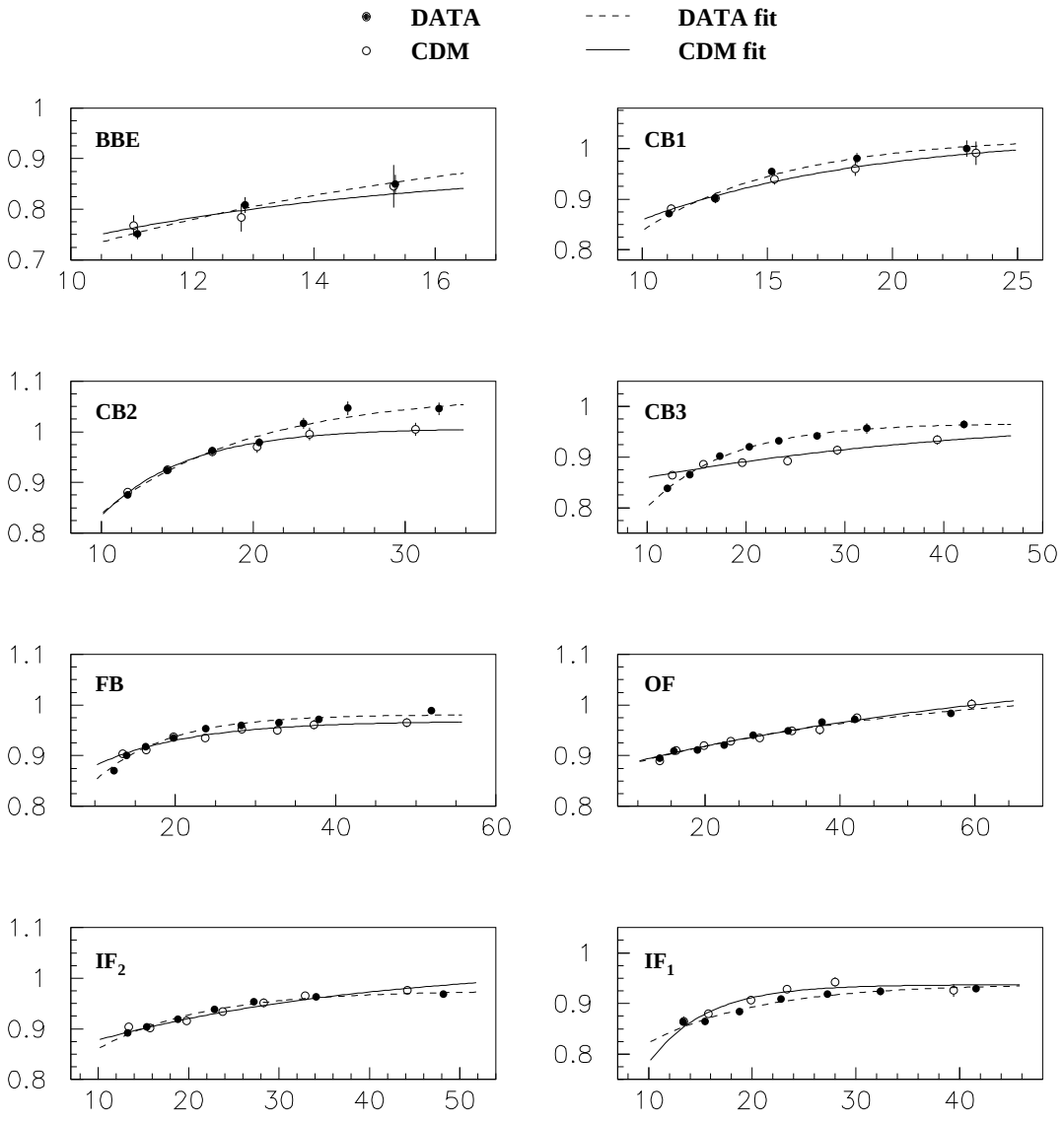

Figure 4: $\mathrm{pt_{had}}/\mathrm{pt_{DA}}$ mean points as a function of $\mathrm{pt_{DA}}$ in the different θ_{jet} regions for data (already corrected by step 1 with respect to CDM Monte Carlo) and CDM Monte Carlo, and the corresponding fitted functions.

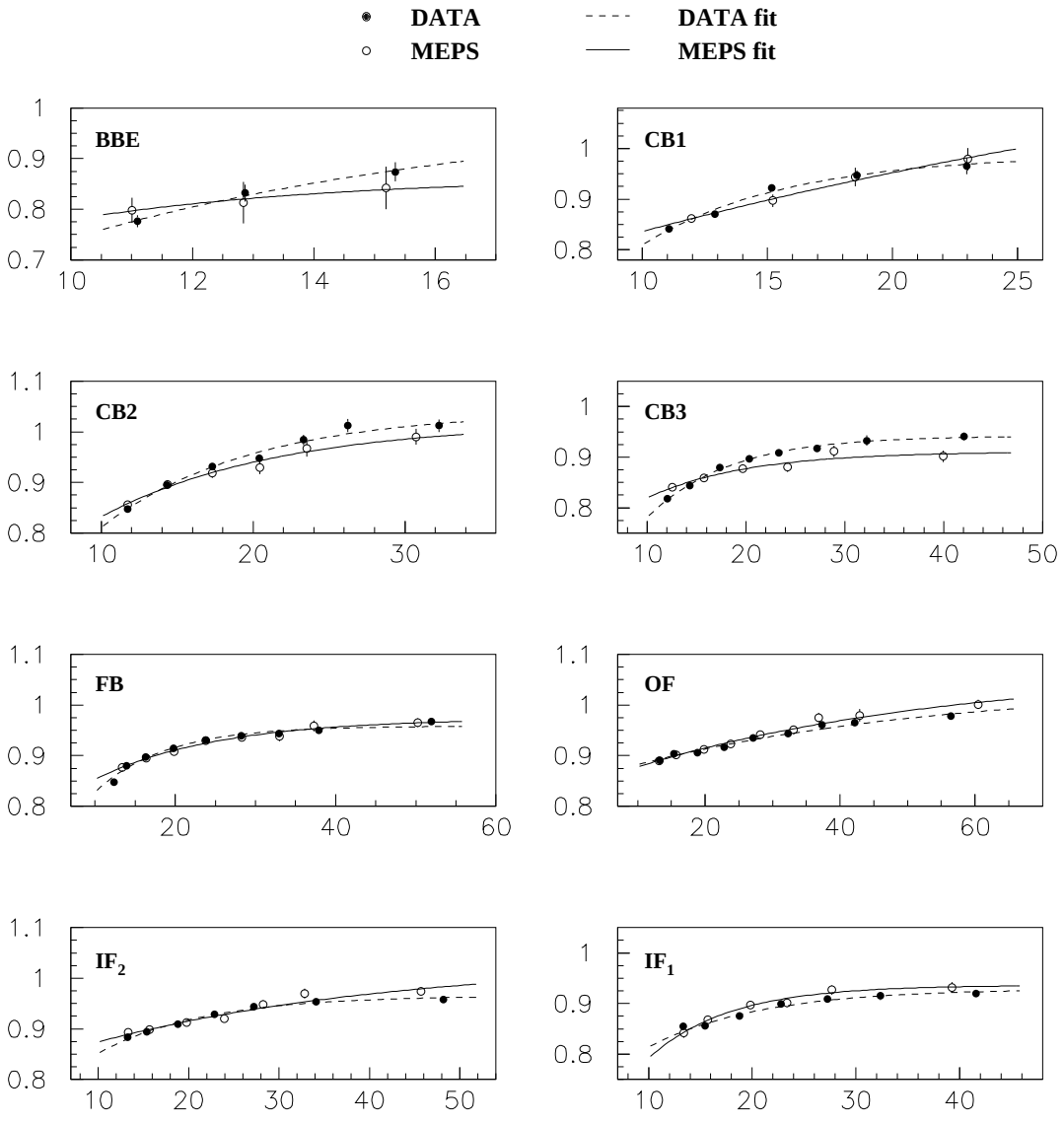

Figure 5: $\mathrm{pt_{had}}/\mathrm{pt_{DA}}$ mean points as a function of $\mathrm{pt_{DA}}$ in the different θ_{jet} regions for data (already corrected by step 1 with respect to MEPS Monte Carlo) and MEPS Monte Carlo, and the corresponding fitted functions.

	wheel	A	B	C	χ^2/ndf
DATA CDM step 1 corrected	BBE	0.9885 ± 0.0830	0 (fixed)	7.7183 ± 1.6075	0.25
	CB1	1.0240 ± 0.0131	0 (fixed)	5.8632 ± 0.2792	1.14
	CB2	1.0757 ± 0.0181	0.5088 ± 0.1358	9.9696 ± 1.6239	1.19
	CB3	0.9670 ± 0.0092	0.5607 ± 0.2248	8.3277 ± 1.4715	0.41
	FB	0.9812 ± 0.0062	0.9135 ± 0.2437	9.0663 ± 1.7039	1.86
	OF	1.0429 ± 0.0188	1.6774 ± 0.0650	44.569 ± 8.1472	2.17
	IF_2	0.9755 ± 0.0086	1.2641 ± 0.2922	11.465 ± 3.2032	0.77
	IF_1	0.9387 ± 0.0115	1.1526 ± 0.3774	10.698 ± 3.6953	1.38
CDM Monte Carlo	BBE	0.8895 ± 0.1187	0 (fixed)	5.6498 ± 2.6240	0.43
	CB1	1.0297 ± 0.0421	0.6960 ± 0.3609	9.0621 ± 3.9590	0.27
	CB2	1.0069 ± 0.0088	0 (fixed)	5.6703 ± 0.2353	0.18
	CB3	0.9858 ± 0.0428	1.7685 ± 0.1736	34.745 ± 17.248	1.29
	FB	0.9685 ± 0.0122	1.5688 ± 0.3812	12.030 ± 5.2670	1.52
	OF	1.0994 ± 0.0901	1.5044 ± 0.2554	66.509 ± 36.468	1.32
	IF_2	1.0294 ± 0.0297	1.5865 ± 0.0766	30.459 ± 10.259	1.38
	IF_1	0.9373 ± 0.0060	0 (fixed)	5.5489 ± 0.2634	1.45
DATA MEPS step 1 corrected	BBE	1.0058 ± 0.0819	0 (fixed)	7.4648 ± 1.5600	0.17
	CB1	0.9884 ± 0.0126	0 (fixed)	5.8472 ± 0.2781	1.14
	CB2	1.0408 ± 0.0174	0.5060 ± 0.1361	9.9386 ± 1.6148	1.20
	CB3	0.9422 ± 0.0089	0.5526 ± 0.2261	8.2721 ± 1.4570	0.39
	FB	0.9584 ± 0.0059	0.8629 ± 0.2474	8.8089 ± 1.6213	2.24
	OF	1.0368 ± 0.0187	1.6775 ± 0.0649	44.486 ± 8.1340	2.15
	IF_2	0.9657 ± 0.0085	1.2641 ± 0.2908	11.497 ± 3.2100	0.78
	IF_1	0.9292 ± 0.0114	1.1517 ± 0.3763	10.702 ± 3.6939	1.39
MEPS Monte Carlo	BBE	0.8644 ± 0.0901	0 (fixed)	4.3202 ± 2.4256	0.04
	CB1	1.3341 ± 0.1221	0.7192 ± 0.1034	37.598 ± 11.385	0.23
	CB2	1.0188 ± 0.0334	0.8348 ± 0.2337	11.596 ± 4.2174	0.64
	CB3	0.9110 ± 0.0175	1.3021 ± 0.5442	10.050 ± 5.5871	0.89
	FB	0.9735 ± 0.0216	1.4410 ± 0.2677	15.362 ± 7.3753	0.46
	OF	1.0706 ± 0.0288	1.5010 ± 0.0777	46.746 ± 10.555	0.71
	IF_2	1.0345 ± 0.0350	1.5642 ± 0.0909	33.523 ± 12.009	1.50
	IF_1	0.9361 ± 0.0123	0.5812 ± 0.4840	7.7584 ± 2.7730	0.54

Table 3: Step 2 : absolute calibration coefficients obtained from the fits of the Fig.4 and Fig.5 points with the function $F(\theta_{jet}, pt_{DA})$. The entry "0 (fixed)" means that the B coefficient is found to be compatible with 0 and therefore is fixed. Also indicated is the χ^2/n.d.f.

3.3 Procedure to apply corrections

The procedure to correct any jet quantity proportional to the energy deposits in the calorimeter is described below.

For a given jet quantity q_{jet} which can be the energy, the px, py or pz momentum components or anything proportional, the notations q_{jet}^{AEFR}, q_{jet}^{rc} and q_{jet}^{corr} stand respectively for uncorrected q calculated at the AEFR level, q corrected by the relative calibration (step 1) and q corrected by the absolute calibration steps (step1 and 2).

The relative calibrated quantity q_{jet}^{rc} is then written as:

$$q_{jet}^{rc} = \frac{q_{jet}^{AEFR}}{Cor_{rc}(\theta_{jet})}$$

where Cor_{rc} are the relative correction coefficients (depending only of the polar jet angle) of section 3.1. Note that for the Monte Carlo's $q_{jet}^{rc} = q_{jet}^{AEFR}$.

The corrected quantity q_{jet}^{corr} is then written as a function of the relative corrected quantity and the absolute correction functions:

$$q_{jet}^{corr} = \frac{q_{jet}^{rc}}{F(\theta_{jet}, pt'_{jet})} \quad \text{where} \quad pt'_{jet} = \frac{pt_{jet}^{rc}}{F(\theta_{jet}, pt_{jet}^{rc})}$$

Note that there is an iteration in this correction procedure. Indeed, the correction functions have been performed as a function of pt_{DA} and what is measured is the hadronic pt_{jet}; thus, the initial pt_{jet} has first to be corrected and then the final corrections are calculated at this corrected pt_{jet} point which is closer to pt_{DA}.

The corrections have to be applied to every reconstructed jet. The calorimeter energy deposits not belonging to a reconstructed jet are not corrected and have just to be added to the quantity under study. This is however only a second order effect as the transverse energy not belonging to any jet is small compared to the total hadronic energy, as shown in Fig.6.

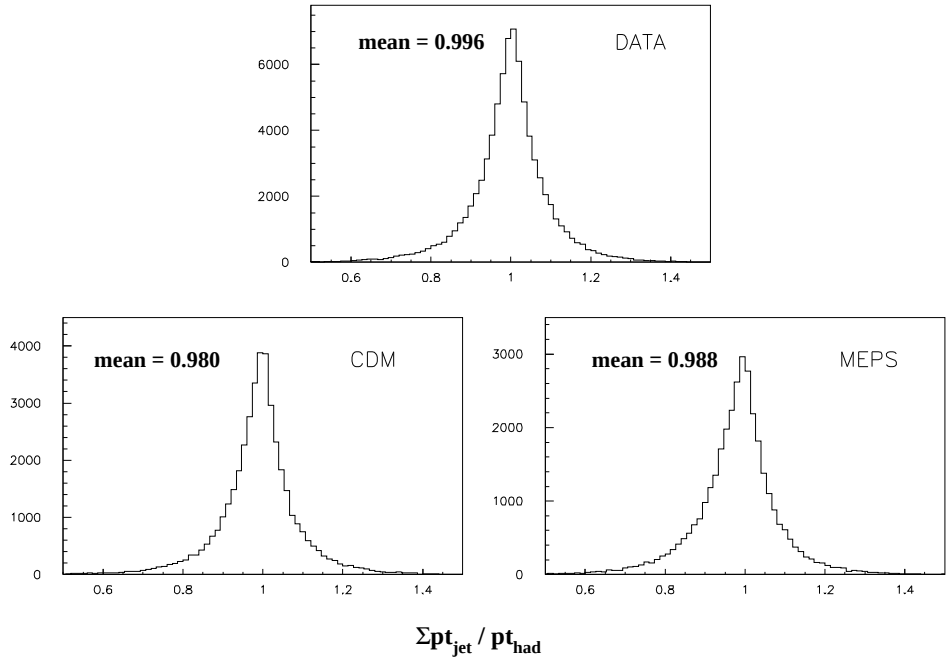

Figure 6: $\sum \mathrm{pt_{jet}}/\mathrm{pt_{had}}$ for the data and Monte Carlo inclusive check samples.

4 Checks of the corrections

In this section, several checks will be discussed after having applied the correction coefficients of Tables 2 and 3 with the procedure described in section 3.3. The selection cuts are the ones used for the checks described in section 2.2.2. In a first part, the necessity of having separated treatment of the two Monte Carlo's is explained. Then, check plots of absolute hadronic energy scale and systematic uncertainties are presented for data and Monte Carlo's.

4.1 Necessity of two different Monte Carlo correction sets

In section 3.2, two calibration sets have been shown for the two Monte Carlo MEPS and CDM models. They are compared in Fig.7(a): this figure shows that, for a given Monte Carlo model, the variation of the transverse momentum of the hadronic system corrected with one calibration coefficient set compared to that corrected with the other calibration coefficient set can be larger than the precision (2%) that one intends to achieve. Therefore, two different corrections have been done.

Fig.7(b) shows the same quantity for the data. As pointed out already in section 3.2, here the two correction sets give the same results for the corrected transverse momentum, because of the step 1 and 2 compensation. In the following, only one of the two correction sets is used to show corrected data quantities.

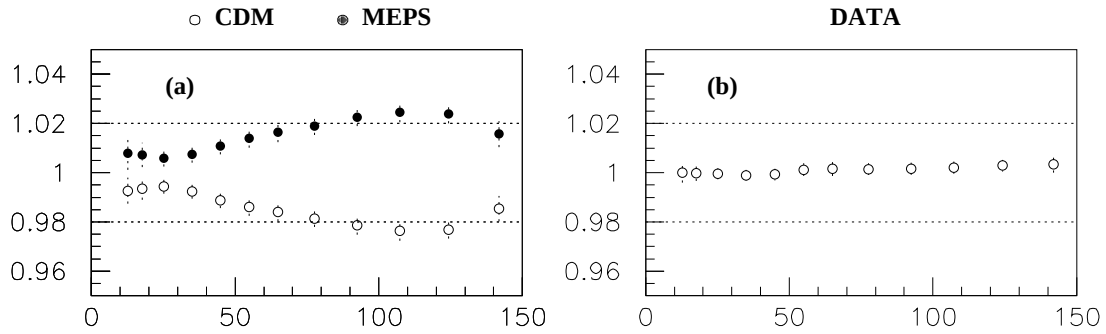

Figure 7: $(\mathrm{pt_{bal}})^{\mathrm{CDM\ coeff}}$ / $(\mathrm{pt_{bal}})^{\mathrm{MEPS\ coeff}}$ versus $\theta^{\mathrm{e}}_{\mathrm{had}}$ for CDM and MEPS Monte Carlo samples (a) and for data sample (b).

4.2 Check with the 1+1 jet check samples

The first check is done with the 1+1 jet samples, i.e. with the events that largely correspond to those used to calculate the correction coefficients, apart from the difference due to the application of the check cuts instead of the calibration cuts. The uncorrected and corrected pt balance distributions are presented in Fig.8. The means of the corrected distibutions are brought close to the unity and the agreements between the data and the two Monte Carlo's are improved as well.

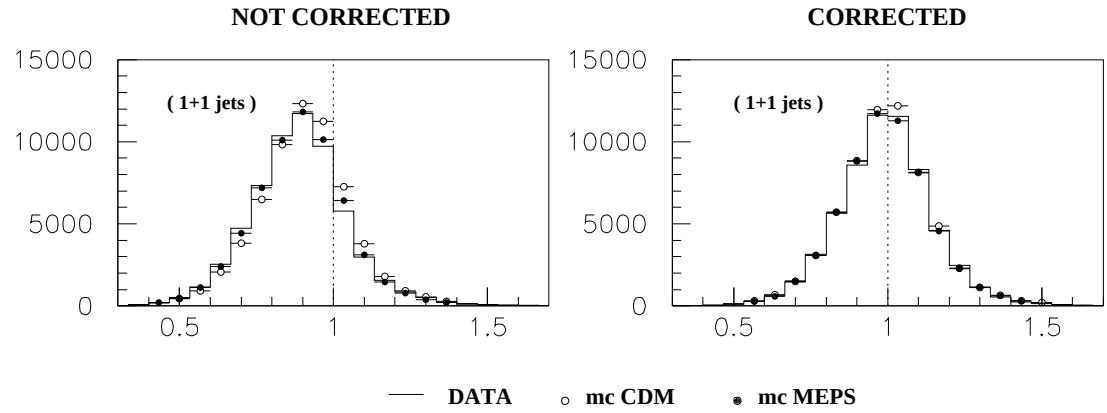

Figure 8: $\mathrm{pt_{had}}/\mathrm{pt_{DA}}$ before and after the hadronic corrections, for data, MEPS and CDM Monte Carlo's having 1+1 jets.

4.3 Checks with independant 1+2 and 1+3 jet samples

The correction functions have been obtained with selected samples containing only 1 jet events (in addition to the proton remnants). Thus, a good check consists to test the calibration with independant samples, i.e. for instance with 2 jet or 3 jet check samples. The uncorrected and corrected pt balance distributions are presented in Fig.9. Again, after corrections, the data and Monte Carlo agreements are improved and the absolute momentum balances are brought around unity.

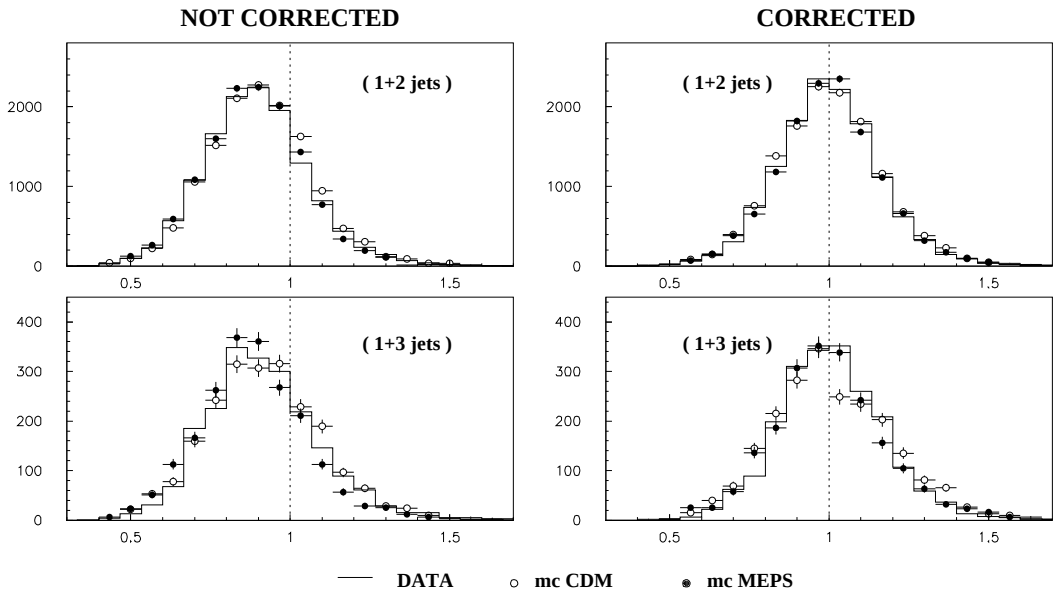

Figure 9: $\mathrm{pt_{had}}/\mathrm{pt_{DA}}$, for 2 and 3 jet event samples, before and after hadronic corrections, for data, CDM and MEPS Monte Carlo's.

Fig.10 shows the pt balance as a function of the transverse momentum and as a function of the inclusive hadronic polar angle θ^{e}_{had}, before and after calibration, for 2 jet data and Monte Carlo samples. The same distributions are presented in Fig.11 for events reconstructed with 3 jets.

From these comparisons, two conclusions can be drawn:

- the absolute hadronic scale is obtained within 2% in all the pt and θ ranges for the data and for the two Monte Carlo's (Fig.10(b), Fig.10(f), Fig.11(b), Fig.11(f)),
- the systematic uncertainties are also smaller than 2% in all the ranges (Fig.10(d), Fig.10(h), Fig.11(d), Fig.11(h)).

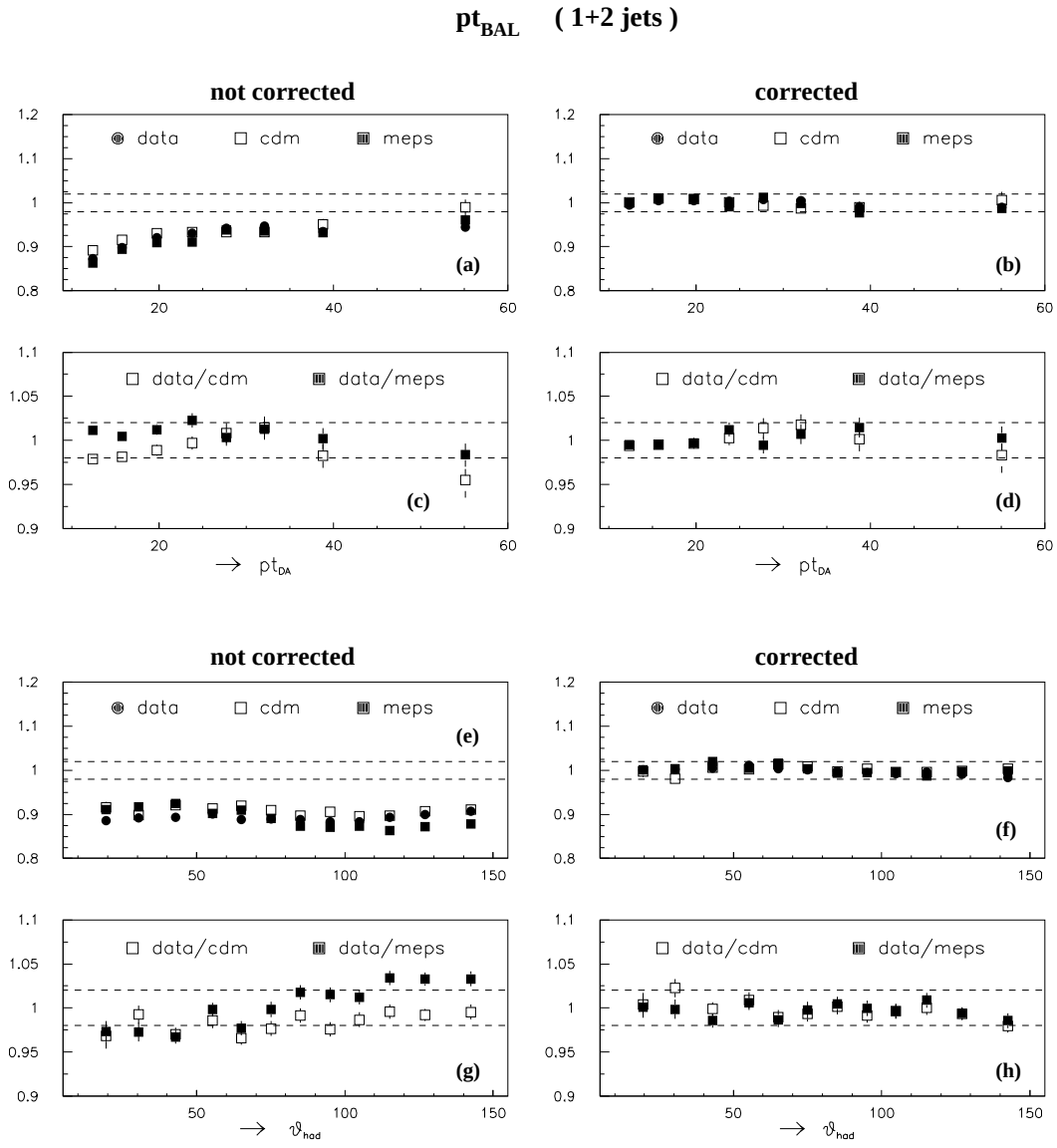

Figure 10: $\mathrm{pt_{had}/pt_{DA}}$ versus pt and versus $\theta^{\mathrm{e}}_{\mathrm{had}}$, for 1+2 jet check samples, before and after hadronic corrections, for data, CDM and MEPS Monte Carlo's [(a), (b), (e), (f)] and for the ratios data/Monte Carlo [(c), (d), (g), (h)].

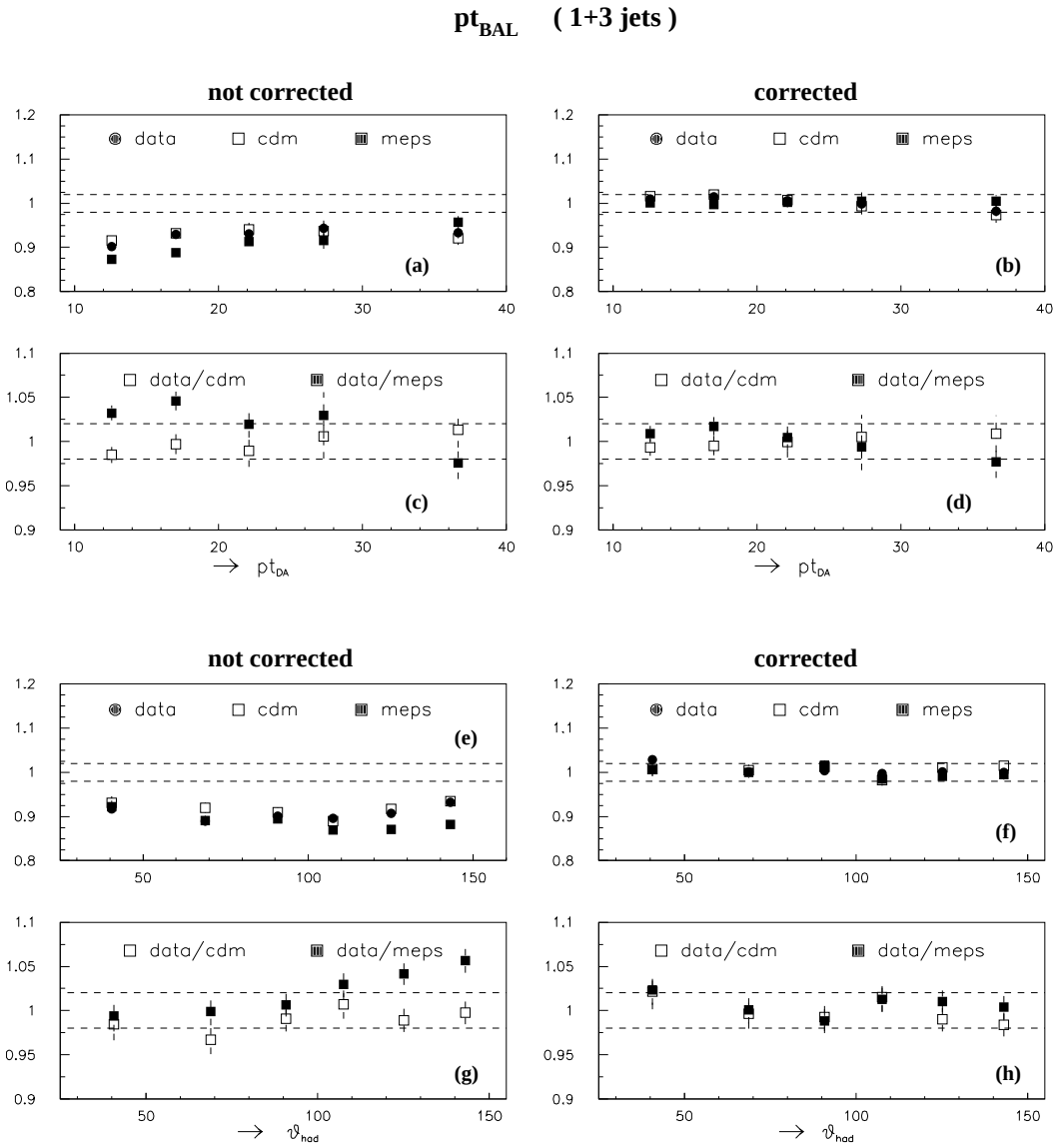

Figure 11: $\mathrm{pt_{had}/pt_{DA}}$ versus pt and versus $\theta^{\mathrm{e}}_{\mathrm{had}}$, for 1+3 jet check samples, before and after hadronic corrections, for data, CDM and MEPS Monte Carlo's [(a), (b), (e), (f)] and for the ratios data/Monte Carlo [(c), (d), (g) ,(h)].

4.4 Checks with the inclusive check samples

With the large inclusive check samples, the calibration can be tested more differentially as a function of the inclusive hadronic polar angle and the transverse momentum at the same time. Although the inclusive samples are dominated by the 1+1 jet events, all events enter in the check ditributions.

Fig.12 shows the uncorrected and corrected transverse momentum balances as a function of $\mathrm{pt_{DA}}$ in each $\theta^{\mathrm{e}}_{\mathrm{had}}$ region.

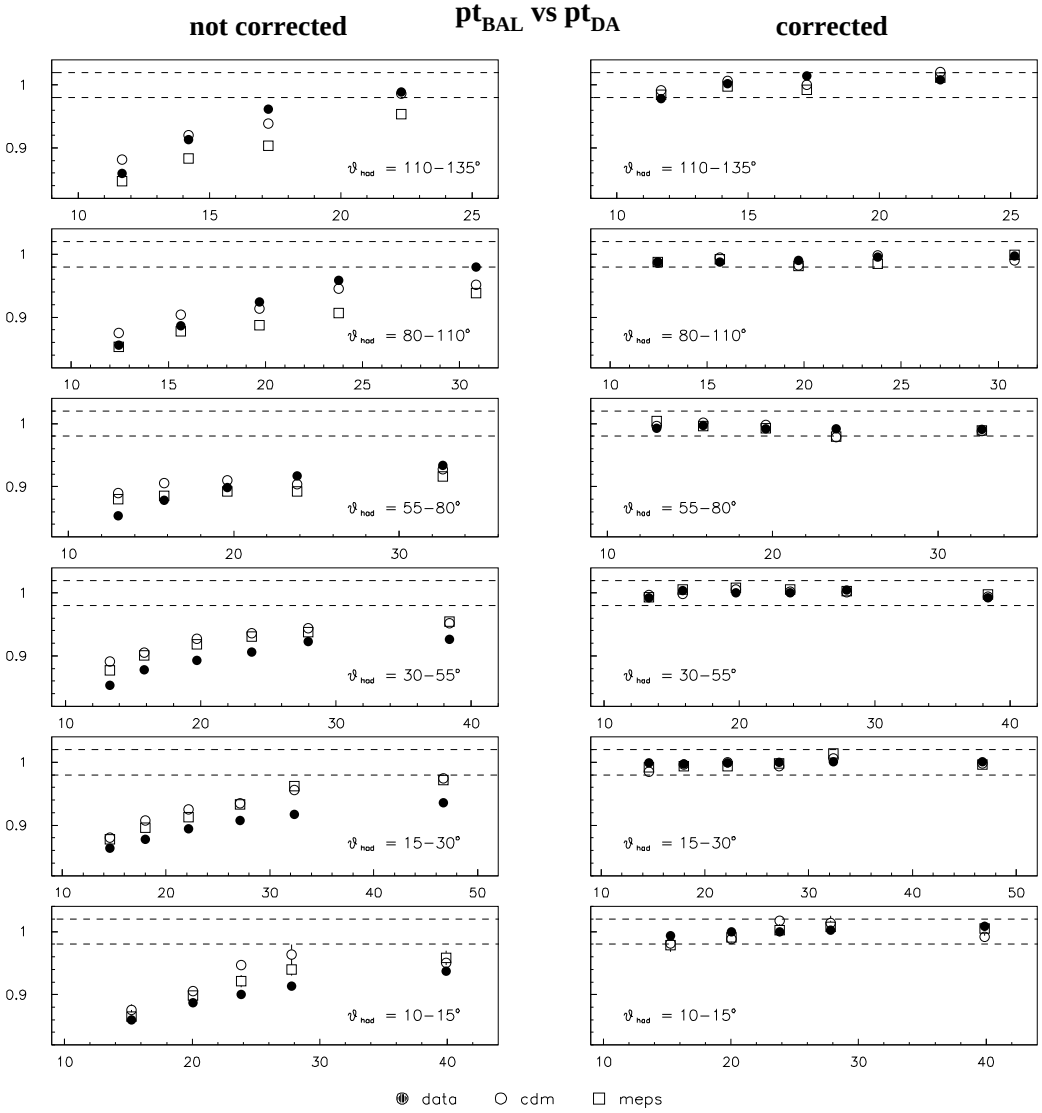

Figure 12: $\mathrm{pt_{had}}/\mathrm{pt_{DA}}$ versus $\mathrm{pt_{DA}}$ before and after hadronic corrections, in the different $\theta^{\mathrm{e}}_{\mathrm{had}}$ regions, for all data, MEPS and CDM events.

The systematic uncertainties are more easily seen with the ratios data/CDM and data/MEPS as shown in Fig.13.

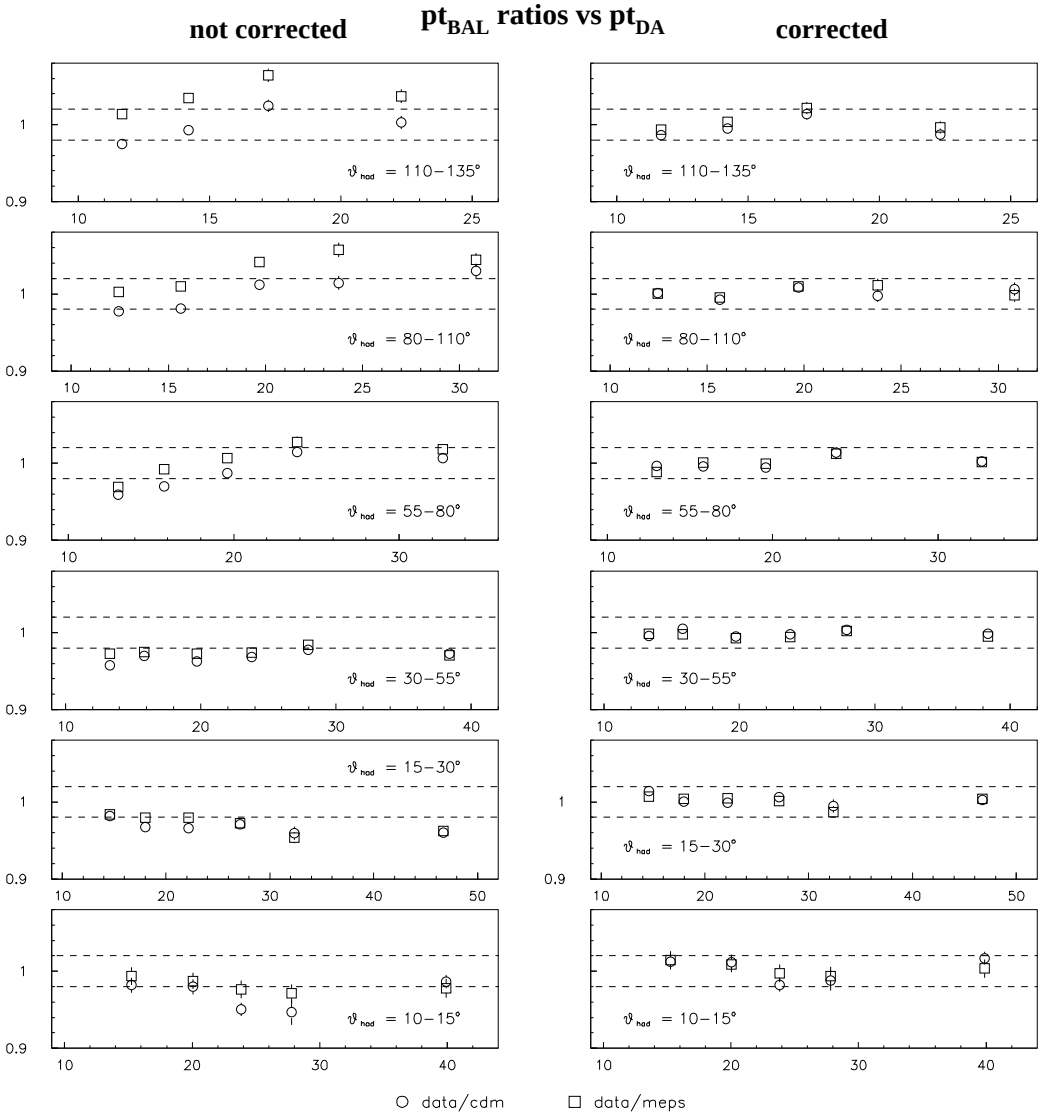

Figure 13: Data and Monte Carlo pt balance ratios versus $\mathrm{pt_{DA}}$ before and after hadronic corrections, in the different $\theta^{\mathrm{e}}_{\mathrm{had}}$ regions, for all data, MEPS and CDM events.

While at the AEFR scale, the hadronic transverse energy is too low by an amount which can reach 20%, after the calibration, the absolute hadronic scale is obtained within 2% in the whole pt and θ range. The systematic differences between data and Monte Carlo's are improved from 5% to 2%.

4.5 Resolution improvements

With the same inclusive check samples, the relative resolutions $\sigma(\mathrm{pt_{bal}})/\mathrm{pt_{bal}}$ calculated before and after applying the hadronic corrections are compared (Fig.14) as a function of $\mathrm{pt_{DA}}$ (left) and as a function of $\theta^{\mathrm{e}}_{\mathrm{had}}$ (right).

These relative resolutions are improved by 5% at high pt and 15% at pt around 10 GeV, and by 10 to 18% in all the θ range. The resolution improvement is mainly due to the fact that at a given $\mathrm{pt_{DA}}$, under-measured hadronic pt's are rescaled by a higher amount than over-measured pt's, due to the decrease of the absolute correction factors with pt.

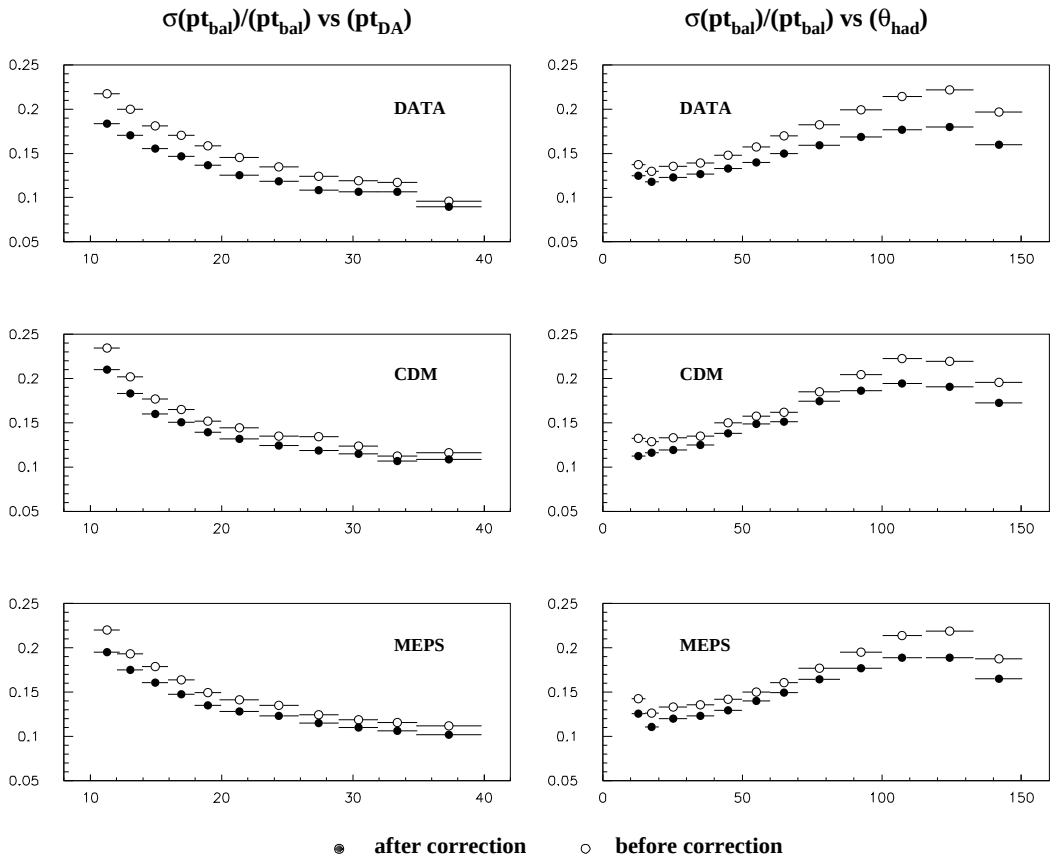

Figure 14: Relative resolutions before and after corrections, for data, CDM and MEPS inclusive check samples, as a function of $\mathrm{pt_{DA}}$ (left) and $\theta^{\mathrm{e}}_{\mathrm{had}}$ (right).

4.6 Jet algorithm independence

In order to check that the calibration method is not dependent on the QJCONE algorithm used to reconstruct the jets, data and Monte Carlo samples have been treated with two other jet algorithms:

- the QJCDFCONE algorithm in which the cone size has been chosen as 1 radian and the minimum transverse jet energy as 4 GeV,
- the JADE algorithm[5] in which the jet resolution parameter $y = m_{12}^2/W^2$ has been set at 0.02, where W is the invariant mass of the hadronic system and m_{ij} the invariant mass of any two objects.

The samples reconstructed with these two algorithms have been corrected with the coefficients calculated previously, i.e. with the coefficients determined with the samples using the QJCONE algorithm.

For the samples reconstructed with the QJCDFCONE algorithm, the corrected distributions are presented in Fig.15(a) as a function of pt and in Fig.15(b) as a function of the inclusive hadronic polar angle for data and Monte Carlo inclusive check samples; the ratios data/Monte Carlo are shown in Fig.15(c) and Fig.15(d).

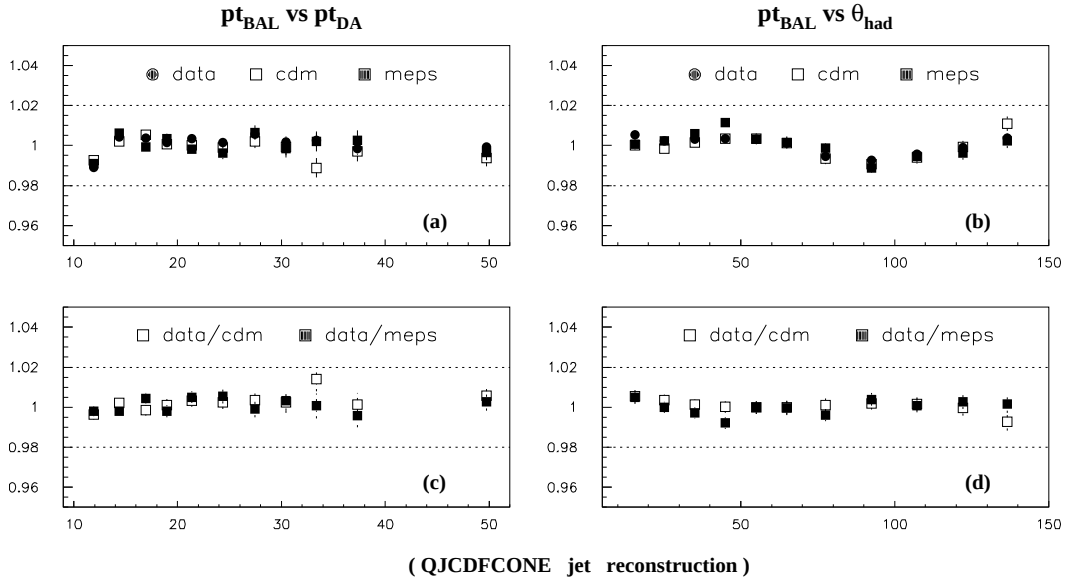

Figure 15: pt_{had}/pt_{DA} versus pt_{DA} (left) and versus θ^e_{had} (right) after hadronic corrections, for data, CDM and MEPS inclusive check samples where jets have been reconstructed with the QJCDFCONE cone algorithm.

The same distributions are presented in Fig.16 for the samples where jets have been reconstructed with the JADE algorithm.

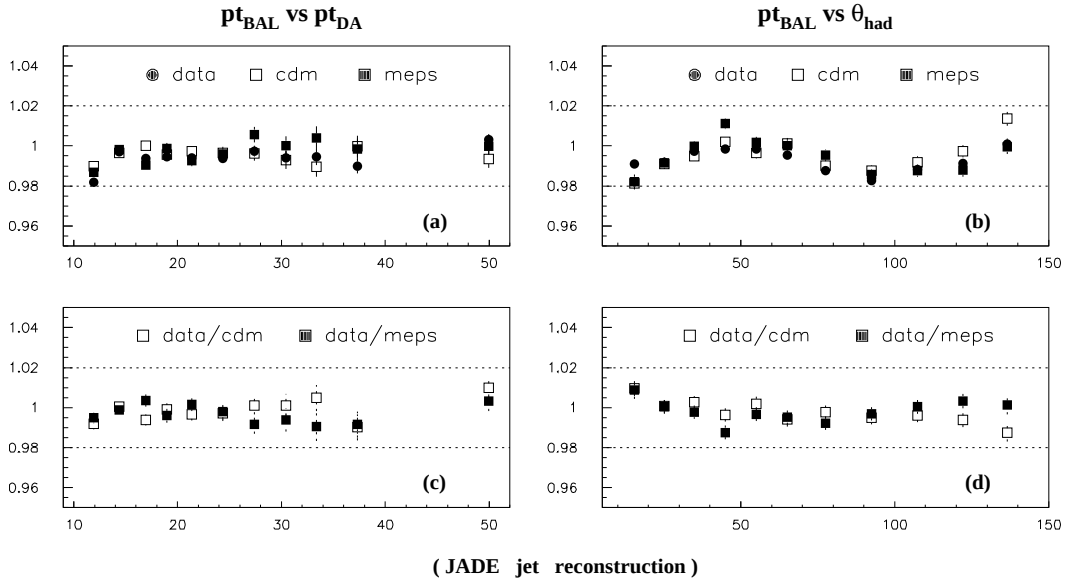

Figure 16: $\mathrm{pt_{had}/pt_{DA}}$ versus $\mathrm{pt_{DA}}$ (left) and versus $\theta^{\mathrm{e}}_{\mathrm{had}}$ (right) after hadronic corrections, for data, CDM and MEPS inclusive check samples where jets have been reconstructed with the JADE algorithm.

The absolute hadronic scale and the systematic uncertainties are good again within 2% in the two sets of distributions; thus, the method is within these errors independent of the chosen jet algorithm.

4.7 y distributions

The effect of the calibration on the quantity E-pz is presented in Fig.17. The distributions show, for data and Monte Carlo inclusive check samples, the uncorrected and corrected $\mathrm{y_{bal}}$ (i.e. $\mathrm{y_{had}/y_{DA}}$) as a function of $\mathrm{y_{DA}}$, where $\mathrm{y_{had}}$ and $\mathrm{y_{DA}}$ are defined as:

$$\mathrm{y_{had}} = \frac{\sum_{\mathrm{h}}(\mathrm{E_h} - \mathrm{pz_h})}{2\mathrm{E_e^0}} \qquad \mathrm{y_{DA}} = \frac{\alpha_{\mathrm{h}}}{\alpha_{\mathrm{h}} + \alpha_{\mathrm{e}}}$$

where α_{h} and α_{e} are the quantities defined in section 2.1.

This $\mathrm{y_{bal}}$ quantity is much improved after the corrections and the 2% level is reached in almost all the $\mathrm{y_{DA}}$ range. The systematic uncertainties, which are of order of 6% at the AEFR level, are below 2% after data and Monte Carlo calibration.

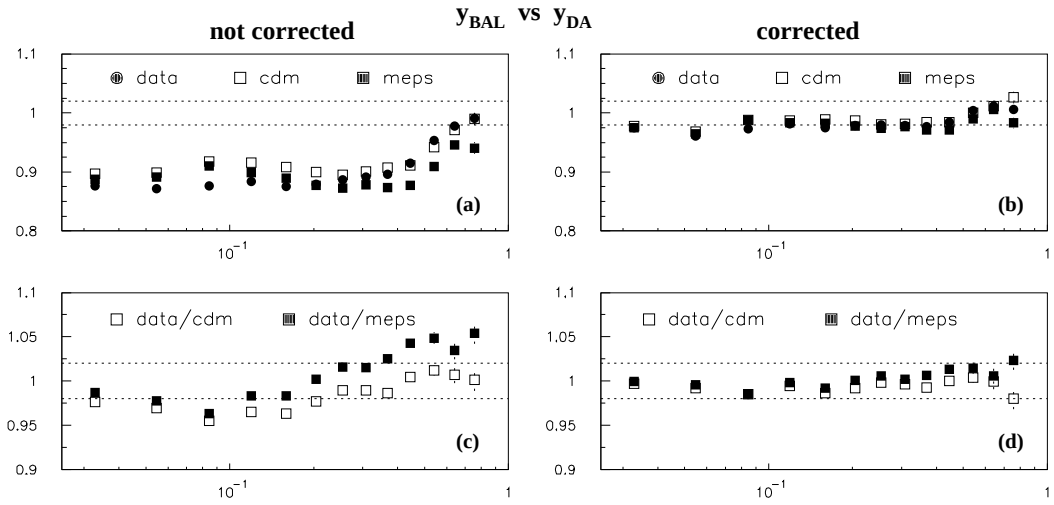

Figure 17: y_{had}/y_{DA} versus y_{DA} for data CDM and MEPS samples.

However, though the ratio y_{had}/y_{DA} is close to unity after calibration, it does not guarantee that the absolute scale is reached for $y < 0.2$. Indeed, as shown in Fig.18, the measurements of y are badly determined towards low y and the hadronic energy scale problem is completely negligible compared to the E-pz measurement errors due to the LAr forward granularity and to noise in the calorimeter.

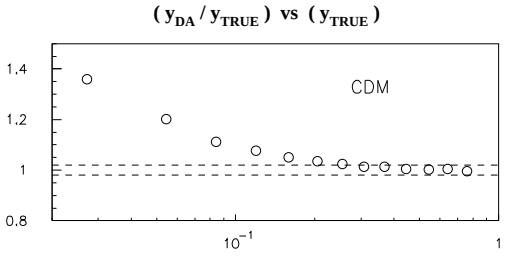

Figure 18: y_{DA}/y_{gen} versus y_{gen} for 1+1 jet calibration CDM sample.

Indeed it is easy to see that the forward Lar finite cell sizes or noise deposits in the barrel of order 1 GeV have small or negligible effects on pt measurements, but can easily change low y values by several 10%. These effects are independent of the energy scale question and not treated in this note.

5 Improvements in an analysis example

The performance of the calibration applied to the charged current event sample, in which only hadronic quantities are available, has also been studied.

In Fig.19 and Fig.20, the stability and the purity obtained in (Q^2, x) bins are compared between the kinematics calculated with the uncorrected AEFR energy

and the calibrated one. The stability (respec. the purity) is defined as the fraction of events which originate from a bin and which are reconstructed in it, divided by the number of generated (respec. reconstructed) events in that bin. In almost every bin, both stability and purity are improved by the hadronic calibration.

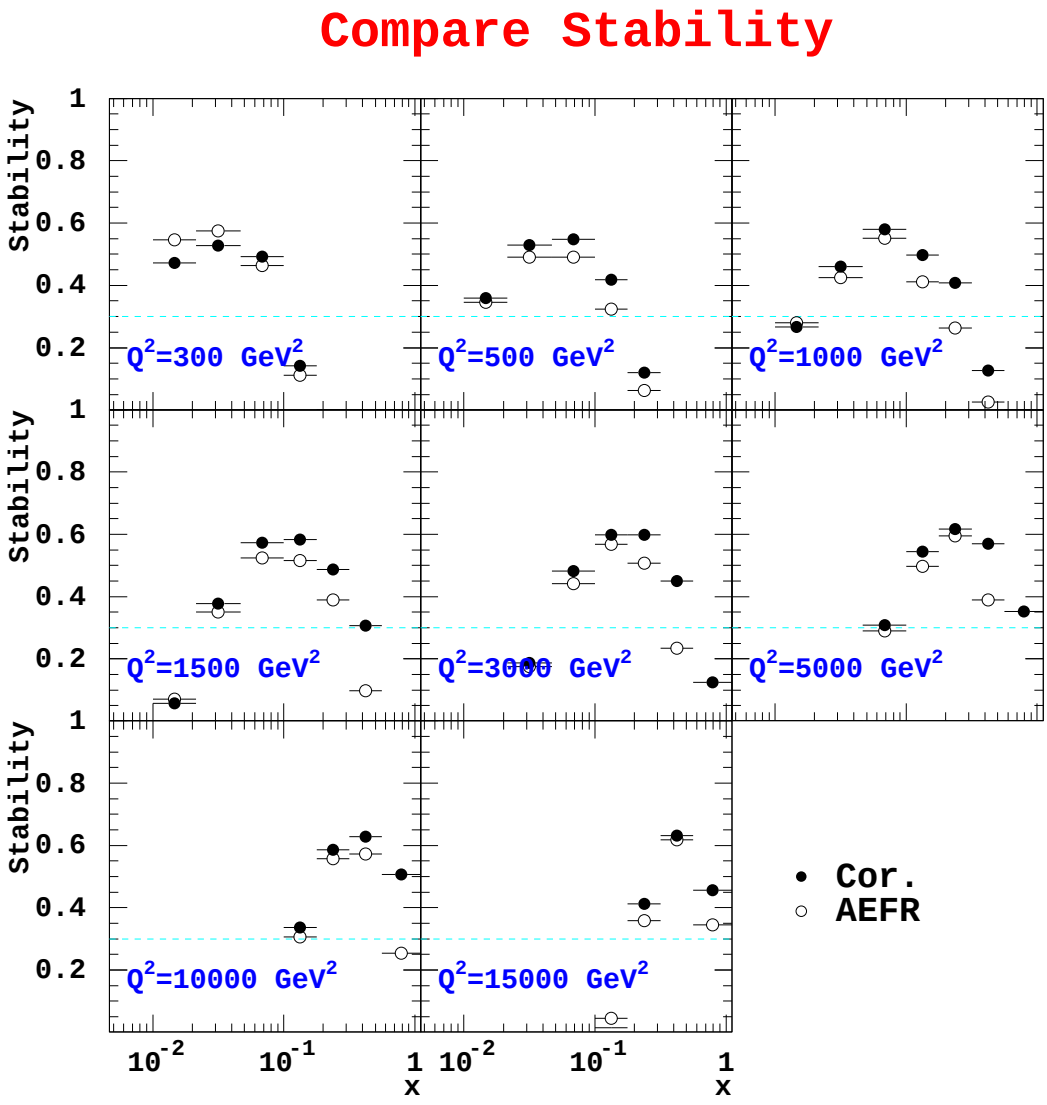

Figure 19: Stability calculated in (Q^2, x) bins for charged current Monte Carlo sample, before (AEFR) and after (Cor.) hadronic corrections.

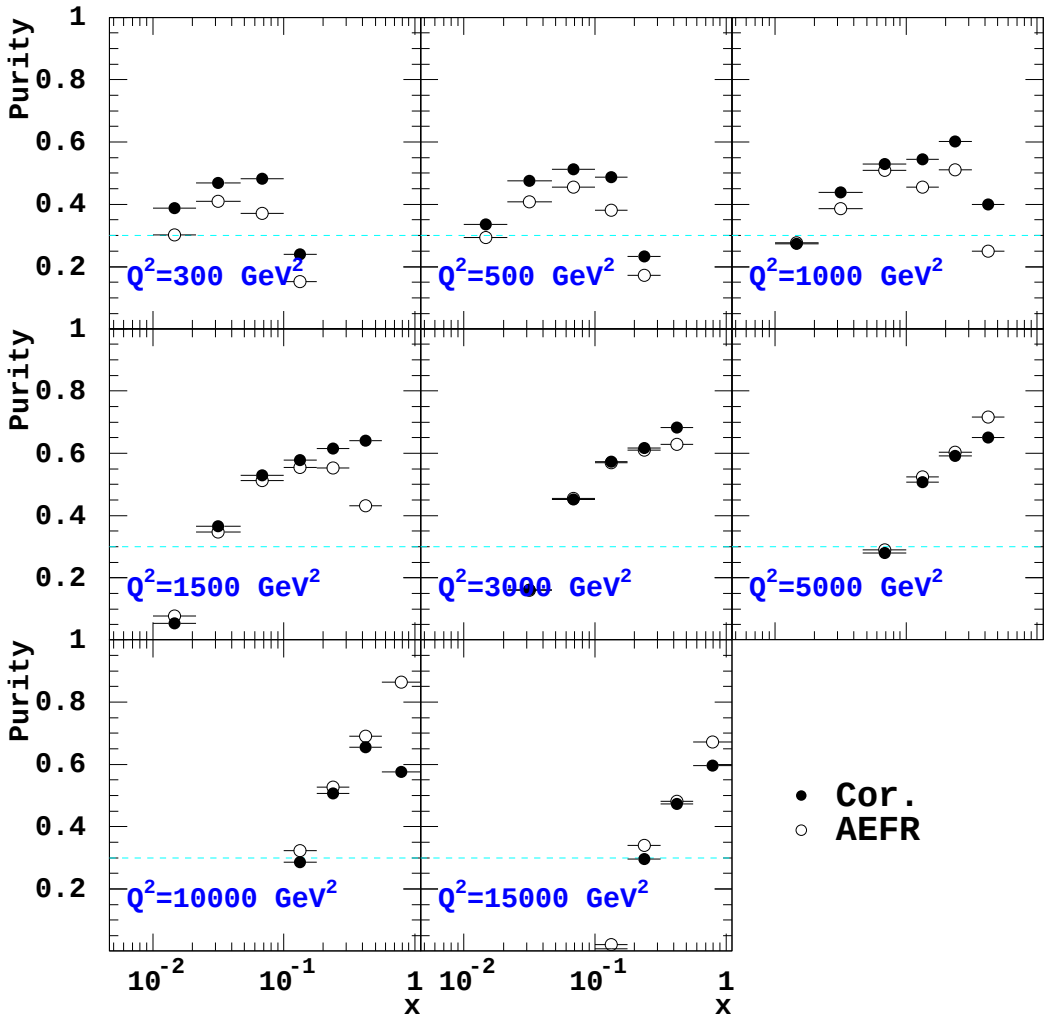

Figure 20: Purity calculated in (Q^2, x) bins for charged current Monte Carlo sample, before (AEFR) and after (Cor.) hadronic corrections.

Using the neutral current data, the "reduced"[6] cross section measured with the Jacquet-Blondel method using the calibrated hadronic system can be compared with other method available for neutral current events, e.g. the double angle method. The comparison shows that the two measurements are in good agreement (Fig.21), which provides a good test for using this calibration for the charged current cross-section measurements.

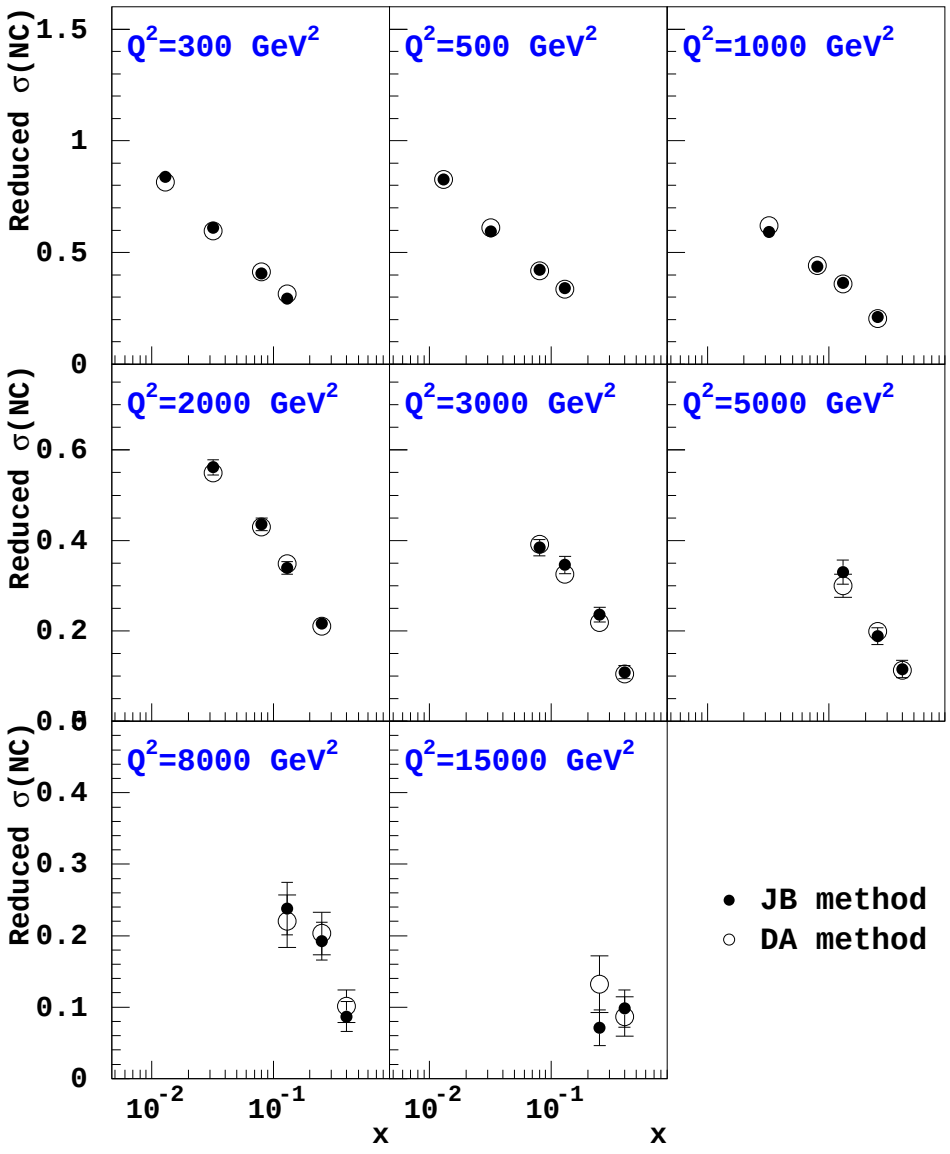

Figure 21: Comparison of the reduced neutral current cross-section measured with the double angle method and the Jacquet-Blondel method.

6 Conclusion

The method described in this note has undergone many cross checks with samples of events having quite different configurations. For an event, the set of corrections to be applied to a measured hadronic energy is given as a function of both the transverse momenta and angles of the jets. The calibration coefficients are applicable for any event samples provided the transverse momentum of either the scattered electron or the hadronic system is larger than 10 GeV. These corrections are within 2% independent of the selection of event samples, of the number of jets in the events, of the jet algorithm used, and of the hadronisation Monte Carlo used for correcting for imperfections of the calorimeter. This method, initially devoted to the absolute calibration of high pt jets (BSM studies or exclusive states) has been shown to work for inclusive studies as well.

References

[1] H.P. Wellisch et al., MPI-PhE/94-03(1994).

[2] L. Lonnblad, Comp.Phys.Comm. **71** (1992) 15.

[3] G.Ingelman, Proceedings of the Workshop Physics at HERA, vol.3, eds. W.Buckmuller, G.Ingelman, DESY (1992) 1366.

[4] J. Kurzhoefer, *The QJCONE jet algorithm and its implementation in H1PHAN*, H1-09/94-375.

[5] JADE Collaboration, W. Bartel et *al*, Z. Phys. **C33** (1986) 23;
JADE Collaboration, S. Bethke et *al*, Phys. Lett. **B213** (1988) 235.

[6] H1 Collab., *Measurements of Neutral and Charged Current Cross-Sections in Positron-Proton Collisions at Large Momentum Transfer*, to be published.

Appendix

The fortran routine **qhadcor.f** which corrects hadronic jets by the method described in this note is currently on the WGS public directory:

/afs/desy.de/user/m/mjacquet/public/hadscale/corrfunc/**qhadcor.f**

The correction function:

qhadcor (**ITYPE**, **theta**, **ptjet**, **qvar**)

correct any jet quantity proportional to the energy deposit in the LAr calorimeter; the INPUT's and OUTPUT variables are described below:

- INPUT's
  - **ITYPE** :
    - 1 for DATA
    - 2 for Monte Carlo in CDM model
    - 3 for Monte Carlo in MEPS model
  - **theta** : polar jet angle in degrees
  - **ptjet** : transverse momentum (calculated at the AEFR scale) of the jet to be corrected.
  - **qvar** : input jet variable to be corrected (any $\propto$ E)
- OUTPUT
  - **qhadcor** : corrected jet variable (any $\propto E_{corr}$)

The implementation of this hadronic jet correction package in PHAN is under study and will hopefully be ready very soon.